View metadata, citation and similar papers at core.ac.uk
brought to you by CORE
provided by Birkbeck Institutional Research Online

# Volumetric budget and grain-size fractionation of a geological sediment routing system: Eocene Escanilla Formation, south-central Pyrenees

**Nikolas A. Michael[1,3], Alexander C. Whittaker[1], Andrew Carter[2], and Philip A. Allen[1,†]**
[1]*Department of Earth Sciences and Engineering, Imperial College London, South Kensington Campus, Exhibition Road, London, SW7 2AZ, UK*
[2]*Department of Earth and Planetary Sciences, Birkbeck College, University of London, Malet Street, London, WC1E 7HX, UK*
[3]*GTT, EXPEC Arc, Building 137, Saudi Aramco, Dhahran, Kingdom of Saudi Arabia*

## ABSTRACT

**The supply of sediment and its characteristic grain-size mix are key controls on depositional facies and stratigraphic architectures in sedimentary basins. Consequently, constraints on sediment caliber, budgets, and fluxes are a prerequisite for effective stratigraphic prediction. Here, we investigate a mid- to late Eocene (41.6–33.9 Ma) sediment routing system in the Spanish Pyrenees. We derive a full volumetric sediment budget, weighted for grain-size fractions, partitioned between terrestrial and marine depositional sectors, and we quantify sediment fluxes between depocenters. The paleo–sediment routing system was controlled by syndepositional thrust tectonics and consisted of two major feeder systems eroding the high Pyrenees that supplied a river system draining parallel to the regional tectonic strike and that ultimately exported sediment to coastal, shallow-marine and deep-marine depocenters. We show significant changes in both the volume and grain-size distribution of sediment eroded from the Pyrenean mountain belt during three different time intervals in the mid- to late Eocene, which controlled the characteristics of stratigraphy preserved in a series of wedge-top basins.**

**The time-averaged sediment discharge from source areas increased from ~250 km$^3$/m.y. to 700 km$^3$/m.y. over the 7.7 m.y. interval investigated. This temporal increase in sediment supply caused major westward progradation of facies belts and led to substantial sediment bypass through the terrestrial routing system to the (initially) marine Jaca Basin. The grain-size mix, measured as size fractions of gravel, sand, and finer than sand, also changed over the three time intervals. Integration of volumetric and grain-size information from source to sink provides an estimate of the long-term grain-size distribution of the sediment supply, comprising 9% gravel, 24% sand, and 67% finer than sand.**

**The techniques and concepts used in the Escanilla study can profitably be applied to paleo–sediment routing systems in other tectonic and climatic settings and to catchments with a range of bedrock lithology and vegetation. This will promote a better generic understanding of the dynamics of source-to-sink systems and provide a powerful tool for forward stratigraphic modeling. The sediment routing system approach has the potential to contribute strongly to new models of sequence stratigraphy.**

## INTRODUCTION

Regions dominated by net erosion, transportation (bypass), and net deposition on Earth's surface are linked by fluxes of particulate sediment within sediment routing systems. Sediment routing systems are integrated, dynamical systems connecting regions of erosion, sediment transfer, temporary storage, and long-term deposition, and they operate from source to sink (Allen and Allen, 2013, p. 226). A key research challenge for sedimentary geologists is to quantify these particulate fluxes and to construct a sediment budget for an entire source-to-sink system. We term the footprint of the paleo–sediment routing system the "fairway," which represents the spatial extent of the sum total of its sediment transport paths and preserved depositional record. Sediment is fractionated during transport (Cross and Lessinger, 1988), principally by selective extraction from surface fluxes to build stratigraphy (Strong et al., 2005; Allen, 2008a; Michael et al., 2013), producing a down-system trend in the relative proportions of grain-size classes and in the mean grain size of gravel (Fedele and Paola, 2007; Duller et al., 2010; Whittaker et al., 2011; Parsons et al., 2012; Michael et al., 2013). Quantification of the sediment budget, its component fluxes, and the down-system evolution of grain size therefore provides essential information to calibrate and test predictive models of basin filling and sedimentary architecture (Paola et al., 1992; Marr et al., 2000; Armitage et al., 2011; Kim et al., 2011).

Erosion and deposition rates, sediment fluxes, and grain sizes can be calculated in modern sediment routing systems using a variety of techniques targeted at short-term observational periods, but these calculated values cannot be easily up-scaled to the longer time scales of geological sediment routing systems (Allen, 2008a; Whittaker et al., 2010). Ancient sediment routing systems, however, are difficult to recognize and investigate: They are likely to be only partially preserved as stratigraphy, making the definition of their fairway problematical; depositional sinks are commonly disconnected from erosional source regions; there may be multiple sources, some of which may be difficult to identify using conventional provenance methods; and the chronological resolution may be inadequate to allow a confident correlation scheme to be developed. Constraining the sediment budget of a geological sediment routing system is therefore a deceptively challenging task, but one that is vital if we are to couple measurements of rock exhumation and erosion rates in mountain belts with realistic estimates of the timing, locus, and magnitude of sediment supply to basins (Sinclair et al., 2005; Beamud et al., 2010; Whitchurch et al., 2011; Carvajal and Steel, 2012; Parsons et al., 2012; Filleaudeau et al., 2012).

Although progress has been made in calculating the sediment fluxes that connect different segments of relatively small, commonly modern or Quaternary sediment routing systems

†E-mail: philip.allen@imperial.ac.uk.

*GSA Bulletin*; March/April 2014; v. 126; no. 3/4; p. 585–599; doi: 10.1130/B30954.1; 11 figures; 3 tables; Data Repository item 2014076;
Published online 3 February 2014.

For permission to copy, contact editing@geosociety.org
© 2014 Geological Society of America; Gold Open Access: This paper is published under the terms of the CC-BY license.

(Covault et al., 2010; Somme et al., 2011; Kim et al., 2011), few workers have targeted larger, buffered systems with well-developed alluvial sequestration (Castelltort and Van Den Driessche, 2003; Allen, 2008b), which make up the bulk of the stratigraphic record. This outstanding challenge is addressed in this paper. We present the sediment budget for the mid- to late Eocene (41.6–33.9 Ma) Escanilla Formation and time equivalents in the southern Pyrenees of northern Spain, which records the late orogenic history of this mountain belt and provides generic insight into the functioning of sediment routing systems in a wedge-top setting. We reconstruct the fairway of the sediment routing system, evaluate its volumetric budget, and determine down-system trends in grain-size fractions from source to sink. Our results provide a benchmark for the downstream fractionation of the total sediment supply in the context of the temporal evolution of a sediment routing system.

## EOCENE ESCANILLA FORMATION

### Geological Background

The Pyrenean mountain belt formed due to oblique collision between the Iberian plate and the European continental margin (Séguret, 1969; Muñoz, 1992; Beaumont et al., 2000), starting in the Late Cretaceous (Puigdefàbregas and Souquet, 1986). Rapid exhumation in the central Pyrenees in the late Eocene–early Oligocene, recognized by thermochronological data (Fitzgerald et al., 1999; Sinclair et al., 2005), caused the delivery of large volumes of coarse conglomerates into the wedge-top region. By the Miocene, the mountain belt was in a state of topographic decay, and these conglomeratic valley fills, fans, and bajadas were incised by headwaters of the Ebro drainage system, occupying the foredeep of the pro-foreland basin system (Coney et al., 1996; Babault et al., 2005; Fillon et al., 2013).

During the Paleogene, the pro-wedge of the mountain belt was characterized by well-developed thrust sheet top (piggyback) basins (Figs. 1 and 2), particularly in the south-central tectonic unit, where the fluvial deposits of the middle to upper Eocene gravel- and sand-rich Escanilla Formation are found (Muñoz, 1992; Puigdefàbregas et al., 1992; Bentham and Burbank, 1996). These wedge-top basins were sourced primarily from the internal zones of the Pyrenees (Sinclair et al., 2005; Whitchurch et al., 2011; Filleaudeau et al., 2012), comprising a stack of south-directed Variscan basement thrust sheets. Fluvial systems in the east supplied deltaic coasts and deep-marine environments in the west during much of the Eocene (Nijman, 1998; Dreyer et al., 1999).

The south-central tectonic unit is bounded to the east by the Segre fault zone and to the west by N-S–trending oblique ramps, including the Boltaña and Mediano anticlines (Fig. 3), termed the Ainsa oblique zone (Muñoz et al., 2013). These anticlines subdivide the south-central region longitudinally into a number of wedge-top subbasins. In an east-to-west transect, the Escanilla-age sediment routing system occupied the Tremp-Graus, Ainsa, and Jaca Basins, whereas the proximal feeder systems were located in the Pobla Basin and northern margin of the Tremp Basin (Figs. 2 and 3). Next, we outline existing geologic and stratigraphic constraints on the Eocene evolution of this paleo–sediment routing system, which provide the framework for our sediment budget analysis.

### Sediment Routing Systems of the Wedge-Top Region

The paleogeography of the south Pyrenean region changed greatly during the mid- to late Eocene interval due to contemporaneous tectonic activity. During the middle-late Lutetian (ca. 44–41 Ma), tectonic shortening allowed deposition of proximal conglomerates in the footwall of the Axial Zone antiformal stack. Fans were confined in their downstream (radial/transverse) extent by the emergence of the Boixols thrust (Fig. 3). The succeeding Pallaresa Group of the Gurb-Pobla area, Cornudella Formation and Sis Groups of the Sis paleovalley, and the Escanilla Formation of the Tremp-Graus and Ainsa Basins mark a significant expansion of fluvial sedimentation and westward progradation of facies belts (Fig. 4), and connection to the Atlantic Ocean in the west was severed at 36 Ma (Costa et al., 2010). In the latest Priabonian (ca. 34 Ma) and continuing into the Oligocene, the wedge-top region was blanketed with coarse-grained fluvial sediment of the Antist (Pobla Basin), Collegats (Sis paleovalley), and Upper Campodarbe (Graus-Ainsa Basins) Groups (Fig. 4).

River systems responsible for the deposition of the Escanilla Formation were confined and guided by the active tectonic structures in the Pyrenean wedge-top region (Fig. 3). These structures were first formed during a southward propagation of thrust displacements, from Late Cretaceous for the Boixols thrust, to Paleocene–late Ypresian for the Montsec thrust, and Lutetian–Oligocene for the External Sierras (Sierras Exteriores/Sierras Marginals) thrust sheet. The topographic expression of thrust-related folds was therefore present by the time of onset of the Escanilla system in the late Lutetian. These thrust-related folds continued to influence the deposition of the Escanilla Formation in the Bartonian–Priabonian, guiding mid- to late Eocene rivers to flow longitudinally, parallel to the wedge-top strike (Bentham et al., 1993; Burbank and Vergés, 1994; Vergés and Burbank, 1996; Burbank et al., 1996; Vergés, 2007; Allen et al., 2013). A magneto-tectonic analysis of vertical-axis rotations in the southern Pyrenees

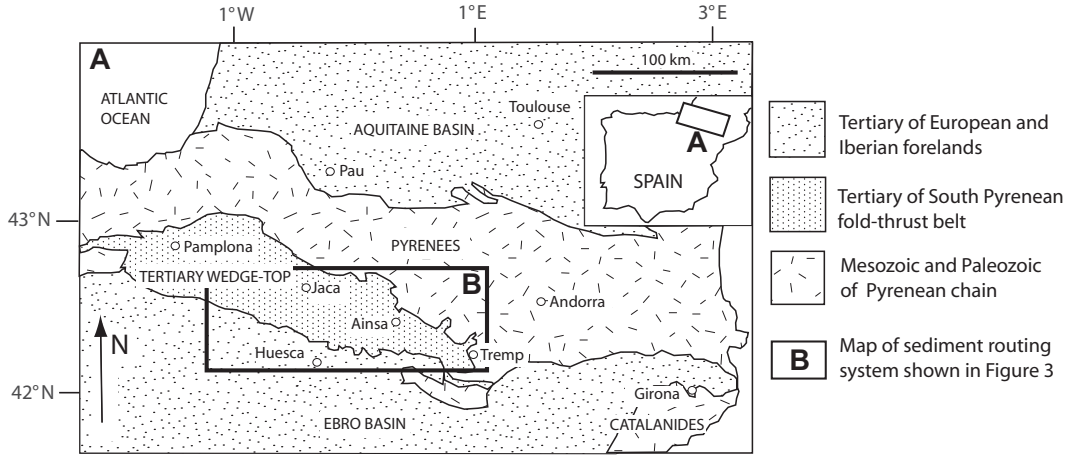


**Figure 1. Location of Pyrenees and Tertiary wedge-top zone. The Aquitaine and Ebro Basins are the retro-foreland and pro-foreland basins of the Pyrenean orogeny, respectively. Box labeled B shows the area occupied by the Escanilla paleo–sediment routing system shown in Figures 2 and 3.**

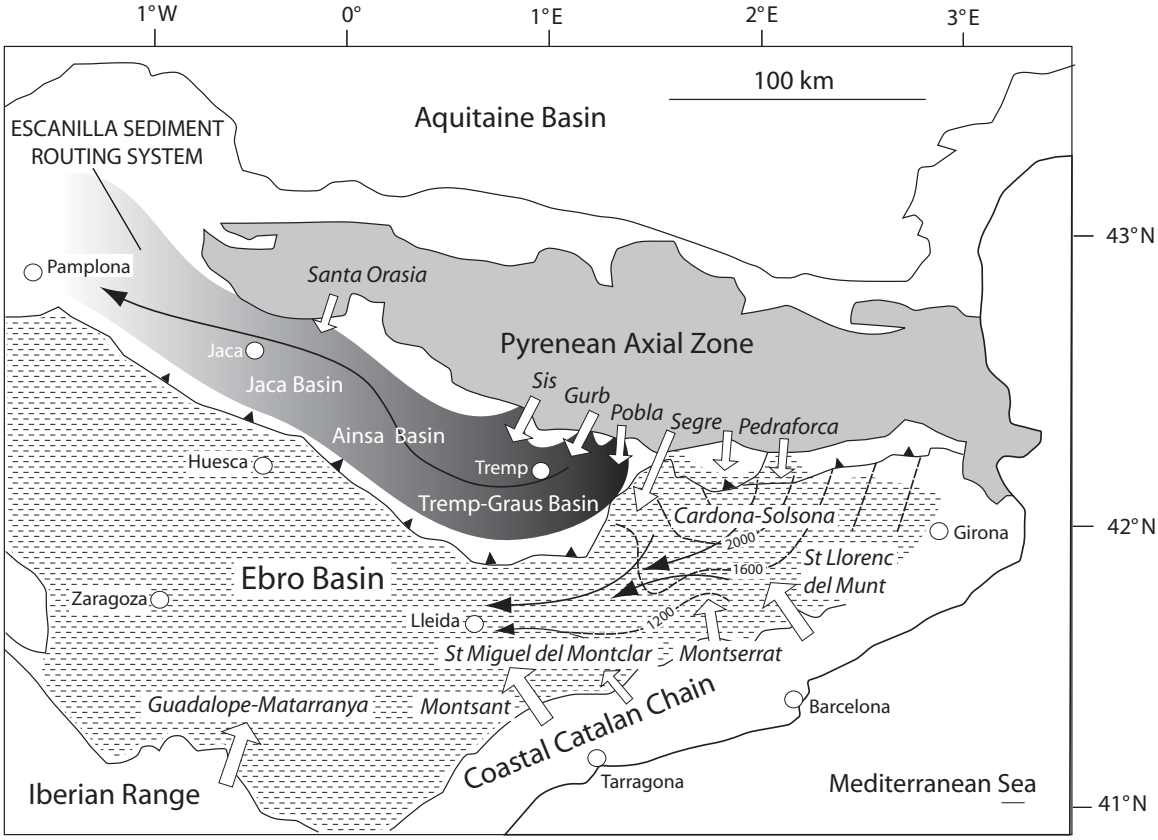


**Figure 2. Major sediment routing systems in the mid- to late Eocene of the south Pyrenean region and its foreland basin system. The Escanilla sediment routing system occupied a wedge-top position and involved the dispersal of sediment toward the west, confined by fold-and-thrust belt structures. The Ebro Basin was fed with sediment from the eastern Pyrenees, the Catalanides, and the Iberian Range. Upper Eocene isopachs (in m) in the northeastern part of the Ebro Basin are from Sinclair et al. (2005). Sediment sources are from Colombo (1980), Allen et al. (1983), Burbank and Vergés (1994), López-Blanco et al. (2000), Ramos et al. (2002), Mellere (1993), Vergés (2007), Sáez et al. (2007), González-Bonorino et al. (2010), and Beamud et al. (2010).**

(Muñoz et al., 2013) showed the periods of activity of the various tectonic structures generating lateral compartments in the contractional wedge-top region. For example, the Mediano anticline started to grow at 48 Ma, and the Boltaña anticline began at 42.5 Ma (Muñoz et al., 2013). All of the lateral structures in the Ainsa oblique zone defining the western limit of the south-central tectonic unit were therefore active in the mid-Eocene by the time of the start of deposition of the Escanilla system.

Although there are substantial thicknesses of middle to upper Eocene sedimentary rocks in the Ebro Basin foredeep and in the fold-and-thrust belt of the eastern Pyrenees (Burbank and Vergés, 1994; Vergés et al., 1995; Garcia-Castellanos et al., 2003; Sinclair et al., 2005), these basin fills were fed from different source regions in the eastern Pyrenees, Catalanides, and Iberian chain and therefore comprise separate, though coeval, sediment routing systems (Fig. 2). This observation is critical to the correct delimitation of the fairway of the Escanilla paleo–sediment routing system (Fig. 3) and to the calculation of a volumetric budget. Sediment delivery from the eastern Pyrenees was blocked from entering the south-central Pyrenean area by the frontal and oblique-lateral folds (Oliana anticline) of the Sierras Marginals thrust sheet.

The maximum length of the Escanilla sediment routing system was >200 km (Fig. 3), including proximal paleovalley and alluvial-fan conglomerates in the Pobla Basin, Gurb escarpment, and Sis area (Mellere and Marzo, 1992; Mellere, 1993; Vincent, 1993, 2001; Whittaker et al., 2011), braided-meandering fluvial/lacustrine deposits in the Tremp-Graus Basin (Lascuarre and Viacamp areas), and braided to meandering channels of the Graus and eastern Ainsa Basins (Bentham and Burbank, 1996; Labourdette and Jones, 2007). The two main sediment sources produced a confluence located near Viacamp (Fig. 3), based on stratigraphic and provenance data (e.g., Vincent, 2001; Michael et al., 2013). The sediments of the terrestrial segment are linked with time-equivalent deltaic, shallow-marine deposits of the Belsué-Atarés Formation of the western Ainsa Basin and deep-marine deposits of the Jaca Basin, represented by the uppermost Hecho Group turbidites and Arguis marls (Hogan and Burbank, 1996; Teixell, 1998; Costa et al., 2010). A subsidiary Pyrenean sediment source for the Jaca Basin compartment of the sediment routing system in the late Eocene is represented by the Santa Orasia fan (Fig. 3; Jolley, 1987).

## METHODS

### Summary

The calculation of a sediment budget for the Escanilla paleo–sediment routing system requires the spatial and temporal connection of proximal alluvial fanglomerates with alluvial plain, coastal marine, and distal marine deposits.

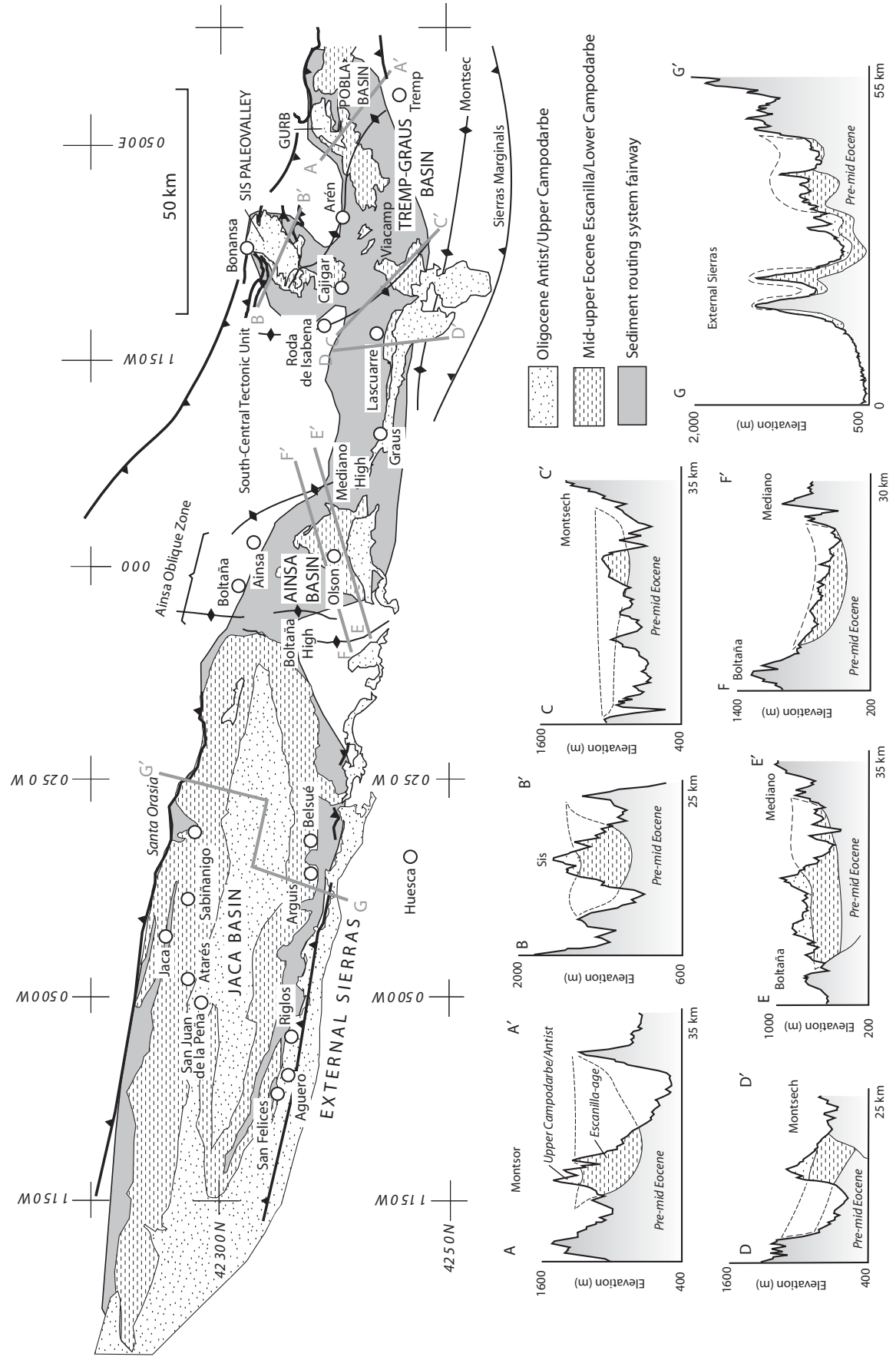


**Figure 3. Map of the Escanilla paleo–sediment routing system from the source areas in the east (Gurb-Pobla and Sis feeder systems), through the Tremp-Graus and Ainsa Basins, to the Jaca Basin in the west. Topographic cross sections along transects A-A′ to F-F′ show the Escanilla Formation and age equivalents. Cross-sectional areas were estimated at each station (Figs. 6 and 7) in the down-system direction and were used to calculate the deposited volumes of the Escanilla sediment routing system.**

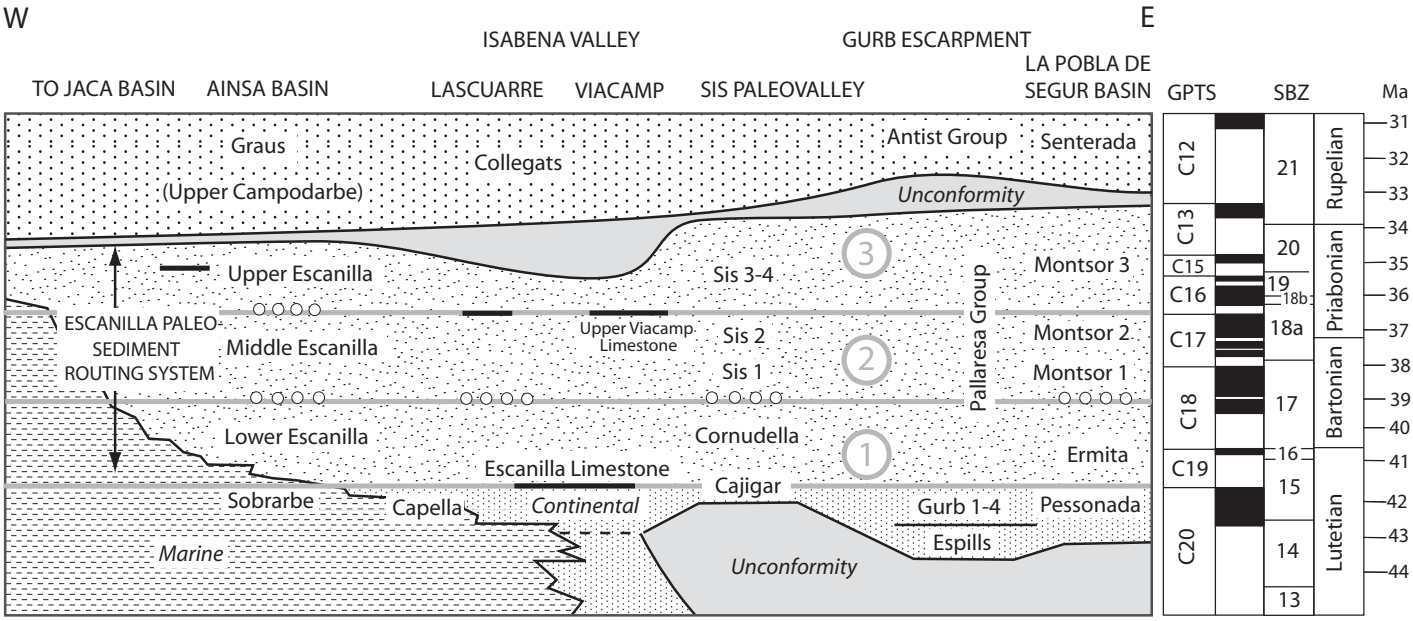


**Figure 4. Chronostratigraphic summary of the mid-Eocene to Oligocene of the south-central tectonic unit of the Pyrenean wedge-top region. Chronostratigraphic information was compiled by Beamud (2013) using sources in Bentham et al. (1992), Bentham and Burbank (1996), López-Blanco et al. (2003), and Mochales et al. (2012) using the time scale of Gradstein et al. (2004). SBZ—larger foraminifera shallow benthic zone; GPTS—global paleomagnetic time scale. Three time intervals within the Escanilla paleo–sediment routing system are from Michael (2013).**

Three time lines were identified (Table 1), spanning the late Lutetian to Priabonian (41.6–33.9 Ma), based on existing biostratigraphic and paleomagnetic constraints (Figs. 4 and 5; Bentham et al., 1992; Holl and Anastasio, 1993; Hogan and Burbank, 1996; Bentham and Burbank, 1996; Beamud et al., 2003, 2010; Costa et al., 2010; Mochales et al., 2012; Rodríguez-Pintó et al., 2012; Beamud, 2013). The dynamic far-field linkage (teleconnection) of coeval deposits along the sediment routing system was established using published geological maps and sedimentary logs supplemented by our own sedimentological logging, paleoflow indicators, and provenance data (clast lithologies, U-Pb dating of detrital zircons, heavy minerals). Time-equivalent data from the Jaca Basin were derived using existing studies (Jolley, 1987; Hogan and Burbank, 1996; Teixell, 1998; Costa et al., 2010). The time lines identified are therefore based on biostratigraphic and magnetostratigraphic correlations, backed up by sedimentological and provenance changes, and are not equivalent to sequence stratigraphic surfaces.

The width of the routing system fairway was mapped from present-day basin width, corrected if necessary for postdepositional erosion of basin stratigraphy (Fig. 6). Measurements of sediment caliber were made at field sites along the trace of this fairway (Fig. 7) for each of the three time intervals. The percentages of gravel (>2 mm), sand (<2 mm and >0.0625 mm), and finer than sand (<0.0625 mm) fractions were calculated at each site by integrating numerous sedimentary logs. The sediment budget of the system was estimated using cross-sectional areas for each time slice derived from our own field observations and published field data (Bentham et al., 1993; Nijman, 1998; Vincent, 2001; Geological Survey of Catalunya and Instituto Geológico y Minero de España [IGME]; digital elevation models [ASTER Program, 2011]). A depositional profile of grain-size fractionation was created for each time interval (Figs. 8 and 9), and the grain-size mix of the entire sediment routing system was calculated by summing the grain-size fraction volumes for all stations.

Deposit volume for each time slice was derived by interpolating between cross-sectional areas at each field station and integrating over the down-system direction. Chemical sediments (primarily carbonates) represent a very small portion of the total sediment volume and can be neglected in the analysis. Their very small volume is incorporated within the grain-size fraction for fines (finer than sand). However, in other cases where autochthonous chemical sedimentary rocks are a significant component of the paleo–sediment routing system, their volume should be estimated and removed from the particulate sediment budget.

Since the porosity of the sedimentary rocks comprising the paleo–sediment routing system is poorly constrained, we neglected this factor in calculating volumes. Consequently, quoted volumes include porosity and are overestimates of the solid volumes making up the three time intervals (Table 2). To incorporate the effects

TABLE 1. THREE TIME INTERVAL SUBDIVISIONS OF THE ESCANILLA PALEO–SEDIMENT ROUTING SYSTEM

| Time interval | Stage | Magnetozone (GPTS)<br>*Biozone (SBZ)* | Age (Ma) | Duration (m.y.) |
|---|---|---|---|---|
| 1 | Lutetian–Bartonian | Base C19–mid C18<br>*Mid SBZ 15–mid 17* | 41.6–39.1 | 2.5 |
| 2 | Bartonian–Priabonian | Mid C18–end C17<br>*Mid SBZ 17–18a* | 39.1–36.5 | 2.6 |
| 3 | Priabonian–Rupelian | Base C16–base C13r<br>*SBZ 18a–end 20* | 36.5–33.9 | 2.6 |

*Note:* Global paleomagnetic time scale (GPTS) magnetozones from Gradstein et al. (2004) and Gradstein and Ogg (2004). Larger foraminifera shallow benthic biozone (SBZ) calibration is from Costa et al. (2010) and Rodríguez-Pintó et al. (2012).

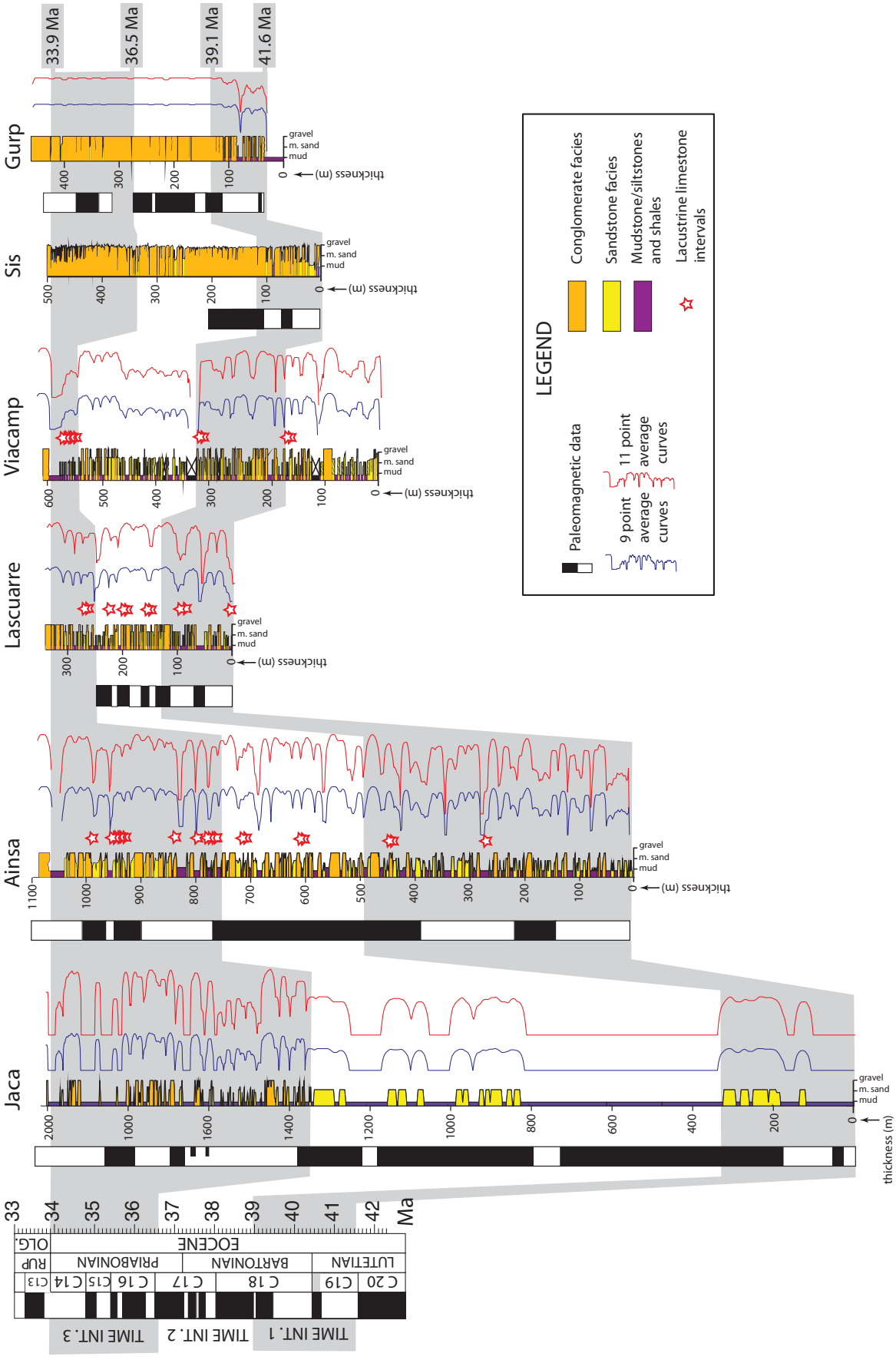


**Figure 5. Correlation scheme based on magnetostratigraphic data, sedimentological marker beds, and provenance signals (Michael, 2013). The stratigraphy is subdivided into three time intervals within a 7.7 m.y. duration of deposition of the Escanilla Formation. This correlation scheme is the framework for the calculation of sediment volumes and grain-size fractions of the Escanilla paleo–sediment routing system. GPTS—global paleomagnetic time scale. Red and blue curves are 11 and 9 point moving averages of grain size.**

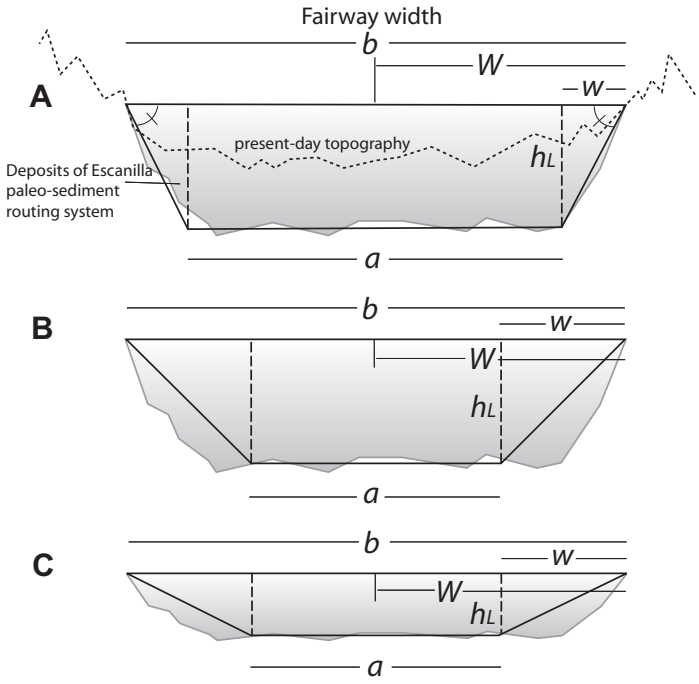


**Figure 6. Isosceles trapezium approximation for a cross section of the Escanilla sediment routing system, showing the impact of stratigraphic thickness $h_L$ and the position of the station relative to the edge of the fairway *w* on the accuracy of the approximation. (A) The station is close to the edge of the fairway (*w* is small), allowing a close approximation to an isosceles trapezium. (B–C) The station is far from the edge of the fairway, making greater errors in assessing cross-sectional area possible. In B, the deposit thickness $h_L$ is large, whereas in C, it is small, with the same width of the lower and upper boundary of the paleo–sediment routing system (*a* and *b*, respectively).**

of porosity in the solid particulate budget, the bulk average porosity of the sedimentary rocks making up the paleo–sediment routing system is required. This information is not available for our study of the Escanilla system.

The sediment supply was estimated for each important tributary (Pobla/Gurb and Sis for time intervals 1 and 2) based on their relative contribution. During time interval 3 in the Jaca Basin, there was an additional important subsidiary source (Santa Orasia), which was taken into account in the calculations. To evaluate the sediment budget of the entire sediment routing system, it was divided into sinks of calculated depositional volume (Sis, Pobla/Gurb, Lascuarre/Viacamp, Ainsa, and Jaca; orange boxes, Fig. 10), together with the connecting sediment fluxes, for each time interval (arrows, Fig. 10; full tabulated data are provided in supplementary material[1]). The ratio of the surface flux of sediment entering each sink compartment versus the deposited flux (both in $km^3$/m.y.) in that sink compartment gives the bypass index.

[1]GSA Data Repository item 2014076, (1) co-ordinates of stations along the sediment routing system, with information on cross-sectional geometry and grain-size fractions; (2) calculated surface sediment discharges and depositional fluxes broken down into grain-size fraction at 10 km steps along sediment routing system, is available at http://www.geosociety.org/pubs/ft2014.htm or by request to editing@geosociety.org.

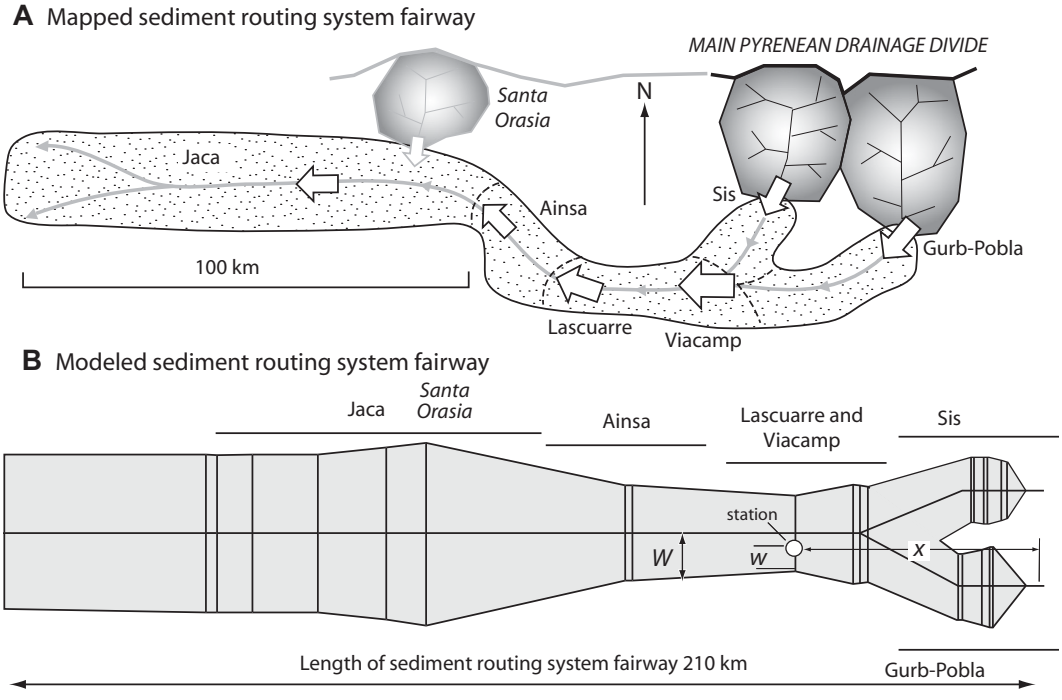


**Figure 7. Stations along the sediment routing system fairway for measurement of sedimentary logs and calculation of grain-size fraction percentages. (A) Schematic view of the entire sediment routing system from source to sink, showing two main feeder systems in the northeast. Santa Orasia is shown as a contributor to the sediment routing system in the late Eocene (time interval 3). (B) Model of the sediment routing system showing locations of stations in the down-system direction (*x*). At each station, a cross-sectional area is estimated using an approximation of an isosceles trapezium. The fairway has a half-width of *W*, and each station is located a distance *w* from the edge of the fairway. The density of station locations is dependent on the distribution of outcropping stratigraphy of Escanilla age (Fig. 3).**

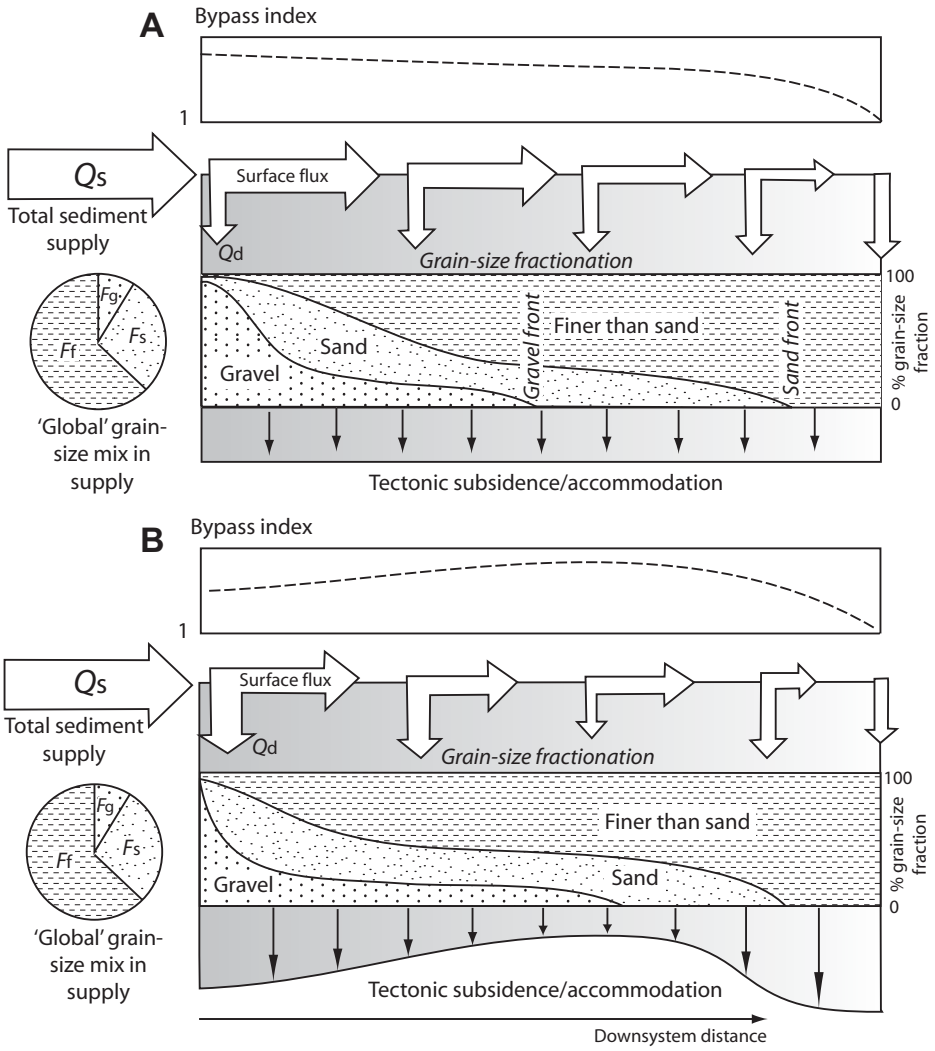


**Figure 8. Schematic diagram to illustrate generic aspects of sediment routing systems. A sediment supply $Q_s$ is composed of grain-size fractions of gravel, $F_g$, sand, $F_s$, and finer than sand, $F_f$. In the depositional realm, tectonic subsidence provides space for long-tem deposition, which causes some of the surface flux of sediment to be selectively extracted to build stratigraphy ($Q_d$). The bypass index at any value of the down-system distance $x$ is the surface flux divided by the depositional flux. Selective deposition causes a distinctive pattern of downstream fining (not shown). (A) A uniform spatial distribution of tectonic subsidence causes $Q_d$ to be everywhere constant, but the surface flux is progressively depleted, leading to down-system exhaustion of first gravel, then sand, and eventually fines. (B) A more complex pattern of tectonic subsidence causes a down-system variation in $Q_d$ and a shift in the position of the gravel front and sand front. For simplicity, the total depositional length, the sediment supply, and the initial size variation in the supply are assumed to be constant.**

Further details on the methods used, especially the justification of the recognition of the three time intervals of the Escanilla system, are provided in supplementary material (see footnote 1). A summary of the methods used for down-system correlation of time intervals within the Escanilla system, the mapping of the fairway, and the likely errors involved is provided next.

## Correlation of Time Intervals

Correlation between localities (Figs. 4 and 5) is based on regional paleomagnetic studies undertaken by Hogan and Burbank (1996) and Costa et al. (2010) in the Jaca Basin, Bentham and Burbank (1996) in the Ainsa and Tremp Basins, and Beamud et al. (2003, 2010) in the proximal paleovalleys and feeder systems of Sis and Gurb. We constructed a correlation panel along the depositional fairway of the sediment routing system and subdivided the stratigraphy into three time intervals representing 41.6–39.1 Ma, 39.1–36.5 Ma, and 36.5–33.9 Ma (Figs. 4 and 5).

Sedimentary graphic logs were constructed from measured sections: Bed thickness, lithology, grain size, sedimentary structures, conglomeratic clast lithology, paleocurrent directions, dip, and dip direction were recorded. The typical resolution of logging was 1 cm to 1 m, since the objective was to capture broad facies relationships, grain size, and facies abundance in the stratigraphic sections in a >200-km-long paleo–sediment routing system. Between three and seven sections were logged in each of five areas—Sis, Gurb, Viacamp, Lascuarre, and Ainsa. These areas can be confidently linked within the sediment routing system based on provenance results from samples collected and field observations, combined with previously published results. Detrital samples were analyzed for apatite fission track (AFT), U/Pb dating of zircons, heavy mineral analysis, inventories of clast lithologies, and paleocurrent data. These data are tabulated in Michael (2013). For the Sis area and the Ainsa and Jaca Basins, detailed sedimentological logs were available from Vincent (1993, 2001), Bentham (1992), Jolley (1987), and Hogan and Burbank (1996).

## Mapping of the Sediment Routing System Fairway

The fairway shows the spatial distribution of the predominantly erosional, transportational, and depositional zones of the sediment routing system. It is based on existing geological maps (Instituto Cartográfico de Cataluña, IGME), Puigdefàbregas (1975), Vincent (2001), Bentham et al. (1993), Labourdette and Jones (2007), Cuevas-Gonzalo (1983), Advanced Spaceborne Thermal Emission and Reflection Radiometer (ASTER) digital elevation models, our own geological field observations, and subsurface data acquired from IGME. Data were collected for the following parameters (Figs. 6 and 7):

$x$ (m) Down-system distance from the point source of sediment (apex of fan)
$W$ (m) Half-width of fairway at a given station
$w$ (m) Orthogonal distance of log locality from nearest edge of sediment routing system fairway
$h_i$ (m) Thickness of the time interval ($i$ = 1–3) at the station
$F_g$ Percentage (fraction) of conglomerate in sedimentary log at a station

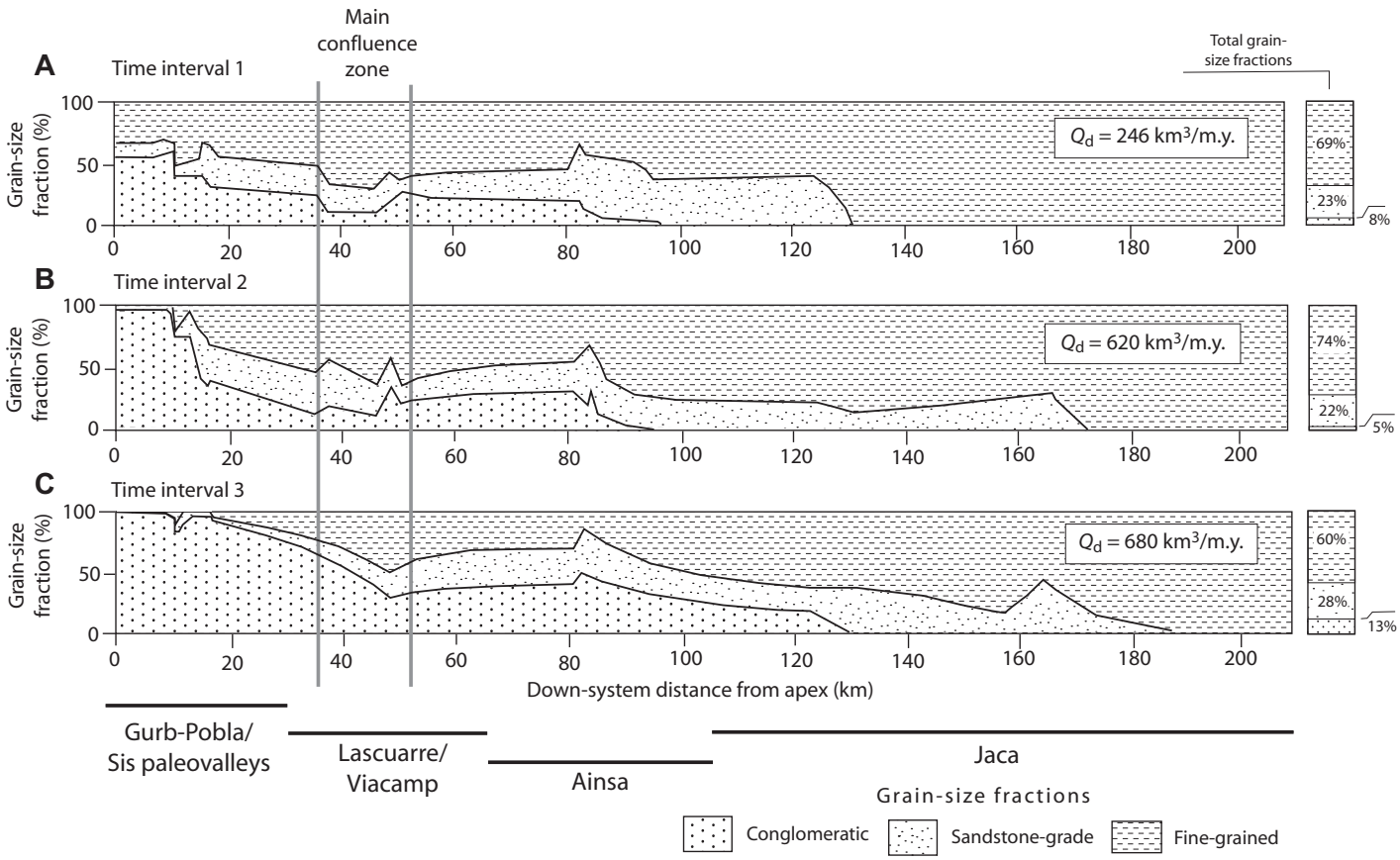


**Figure 9. Grain-size fractions of gravel, sand, and finer than sand in percent (%) against down-system distance from the depositional apex for the Escanilla sediment routing system for (A) time interval 1, (B) time interval 2, and (C) time interval 3. The right-hand bar shows the overall grain-size fractions released to the system as a proportion of the total sediment volume for that time interval. $Q_d$ is depositional flux in km³/m.y. The "global" grain-size mix released from Pyrenean catchments during the mid- to late Eocene, based on the grain-size fractions measured in the Escanilla paleo–sediment routing system for intervals 1, 2, and 3 combined, is 9% gravel, 24% sand, and 67% finer than sand.**

$F_s$ Percentage (fraction) of sandstone at a station

$F_f$ Percentage (fraction) of fines (finer than sand and limestones) at a station

Cross-sectional areas were calculated using simplified geometric shapes (e.g., triangle, rectangle, isosceles trapezium) and subdivided according to area occupied by each size fraction ($F_g$, $F_s$, $F_f$). Interpolation between localities allowed depositional volumes subdivided by size fraction to be estimated in the down-system direction. The results presented here are based on the isosceles trapezium approximation (Fig. 6), which is believed to be the closest geometrical shape to the Escanilla Formation and age equivalents and is easily implemented (see supplementary material [footnote 1]).

The percentage of a grain-size fraction making up the stratigraphy as a function of down-system distance (Fig. 9) shows the overall downstream fining over the 210 km length of the paleo–sediment routing system. The total volumes occupied by each grain-size fraction give the total sediment grain-size mix and the total volume of sediment released by upstream catchments (Figs. 8 and 9). Since sediment cascades from source to sink, the volumetric profiles also make possible the estimation of the depositional fluxes at each station and the remaining surface flux. In this way, the transfer of surface sediment fluxes from station to station or from sink compartment to down-system compartment becomes evident (Figs. 10 and 11).

## Errors

A summary of possible sources of error is given in Table 2. The parameters in the input data that involve the least amount of error are parameters $x$ and $h_i$. The horizontal distance from the point source $x$ was measured using ArcGIS (ESRI). Stations were located by global positioning system (GPS) using a Garmin Oregon 550 with a centimeter to meter accuracy, representing negligible error. The thickness derived from sedimentary logs for each time slice, $h_i$, also carries little error. Most sedimentary logs were constructed with meter-by-meter accuracy at the coarsest resolution, translating to a few meters error per 100 m of section in worst cases, which propagates linearly to the volumetric calculations. We estimate a maximum of 3% error in volume calculations.

Errors in volumetric calculations derive principally from the mapping of the fairway. In the Tremp and Ainsa Basins, the fairway was delimited confidently, since the system was structurally confined by the Montsec, Boixols, Turbon, Mediano, and Boltaña structural culminations. An error of 1000 m on either side of the boundary of the fairway is estimated, equating to an allowable 2 km of error in delimiting the boundary of the system. This is an error of ~5% in volume calculations. In the Jaca Basin, however, the limits of the fairway are more speculative.

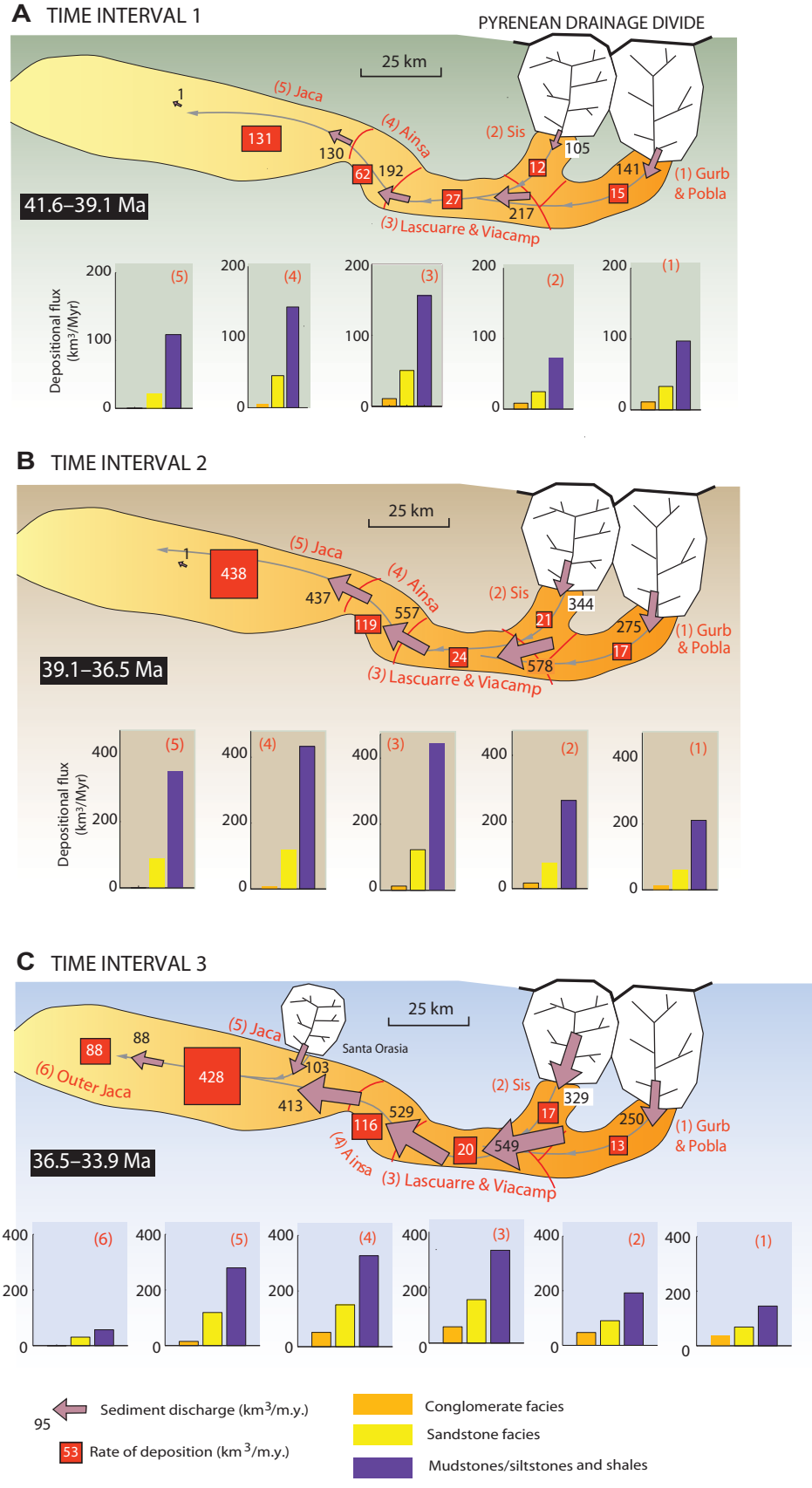


**Figure 10. Summary of sediment fluxes (purple arrows) and depositional fluxes (red boxes) for the Escanilla sediment routing system. Arrows and boxes are sized proportionally to the magnitude of the discharge (km³/m.y.) and volumetric depositional flux (km³/m.y.). Sectors for fluxes and sinks are (1) Gurb/Pobla system; (2) Sis paleovalley; (3) Lascuarre and Viacamp; (4) Ainsa Basin; (5) inner Jaca Basin, (for time interval 3 only); and (6) outer Jaca Basin. Histograms show grain-size fractionation for each compartment of the sediment routing system in terms of the depositional flux in km³/m.y.**

Estimates of fairway width (or half width, $W$) are based on structural cross sections and palinspastic reconstructions from Jolley (1987), Teixell (1998), and Turner (1992), leading to a value of 4000 m in the possible error in delimiting the fairway boundaries, or ~10% error in volume calculations.

Further errors derive from the isosceles trapezoid approximation for cross-sectional area (Fig. 6). Based on seismic and structural cross sections, this shape provides a good representation of the subsurface shape of the stratigraphic fill. Errors originate from the calculation of the basal width of the cross section $a$, and they become greater with the thickness of the time interval $h_i$ and with the distance of the station relative to the boundary of the fairway, $w$ (further discussion in supplementary material [see footnote 1]). Errors in the isosceles trapezoid approximation are likely to cause underestimations of cross-sectional areas, but they are unsystematic and difficult to quantify without precise subsurface imagery.

The chronology used is principally based on paleomagnetic zonation (Bentham et al., 1992; Beamud et al., 2003, 2010; Mochales et al., 2012; Rodríguez-Pintó et al., 2012) calibrated to the global paleomagnetic time scale (Gradstein et al., 2004). Periods of normal and reversed polarity within a paleomagnetic zone range from $<10^5$ yr to 1 m.y. The worst case error is therefore ±0.5 m.y. in terms of age assignment.

What is the ideal time duration for subdivision of the paleo–sediment routing system? (1) The time intervals should be short enough to reflect genuine changes in the functioning of the system under external forcing and internal dynamics; (2) the time intervals should be long enough to permit basinwide correlation and an averaging of facies and grain-size characteristics; (3) the time intervals should be long enough that lower and upper boundaries do not fall within a single chronological zone. Since

TABLE 2. ESTIMATE OF THE VARIOUS POSSIBLE ERRORS IN THE ANALYSIS

| Source of error | Estimate | Notes |
|---|---|---|
| Bulk porosity | <10% overestimate of total volume | Depends on lithology and maximum depth of burial |
| Chemical sedimentary rocks | <2% overestimate of fine fraction and total sediment volume | Three-dimensional extent of carbonates is unknown; estimate is based on abundance of carbonate beds in sedimentological logs |
| Horizontal coordinate $x$ | Negligible | |
| Vertical thickness $h_i$ | ±3% in volume calculations | Most uncertainty in time interval 3 |
| Mapping of sediment routing system fairway | 5%–10% in volume calculations, most likely underestimate | 5% in Pobla-Tremp-Graus-Ainsa Basins, 10% in Jaca Basin |
| Cross-sectional areas | Unknown, but underestimate of total volumes | Derives from isosceles trapezium approximation |
| Magnetochronology | Worst case ±15% in volume calculations for total sediment volume of Escanilla paleo–sediment routing system | Up to ±0.5 m.y. uncertainty in age assignments |

*Note:* Some errors lead to underestimates, while others lead to overestimates of sediment volumes.

catchment-fan systems appear to respond to step changes in drivers over periods of ~1 m.y. (Densmore et al., 2007; Armitage et al., 2011), the duration of magnetozones ranges up to 1 m.y., and the time scale for statistical averaging of sediment properties is $>10^4$ yr (Duller et al., 2010), a minimum time duration for "slicing" of the sedimentary rocks of the sediment routing system is of the order of a million years. The three time intervals recognized in the Escanilla paleo–sediment routing system are 2.5–2.6 m.y. in duration. A higher-resolution slicing may be possible in cases of very high-quality chronology. It is worth noting that the time intervals are similar to the typical duration of depositional sequences.

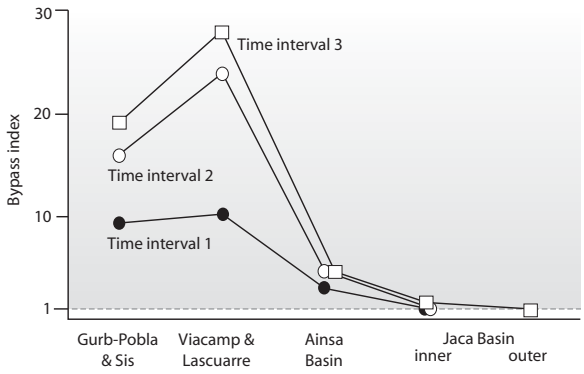


**Figure 11. The bypass index for the three time intervals of the Escanilla system in the down-system direction. The bypass index is the ratio of the incoming surface sediment flux for a basin compartment to the depositional flux in that compartment. In all time intervals, there is a similar down-system trend in bypass and a secular increase in the amount of bypass for each basin compartment.**

TABLE 3. SUMMARY OF TOTAL SEDIMENT VOLUMES FOR TIME INTERVALS 1 TO 3 AND VOLUMETRIC FRACTIONS OF GRAVEL, SAND, AND FINES

| Interval | Total volumes ($km^3$/m.y.) | Volumetric fraction gravel (%) | Volumetric fraction sand (%) | Volumetric fraction fines (%) |
|---|---|---|---|---|
| 1 | 246 ± 20 | 8 | 23 | 69 |
| 2 | 620 ± 48 | 5 | 22 | 73 |
| 3* | 682* ± 61 | 13 | 27 | 60 |

*Note:* Uncertainties are given for total sediment volumes per m.y. Volumes are uncompensated for porosity.
*The total volume for time interval 3 does not take into account the recycling of some of this interval by erosion at the sub-Oligocene unconformity. A volume of ~80 $km^3$ was removed by erosion, based on the area affected and the thickness of time interval 3 sedimentary rock thought to have been removed. The corrected total volume for time interval 3 is therefore approximately 713 when expressed in $km^3$/m.y.

## RESULTS

For each time interval, the total cumulative volume in the downstream direction and its breakdown into grain-size fractions illustrate both the grain-size mix of the sediment supply and the depositional dynamics of the sediment routing system. Total depositional volume per million years increased throughout the study period from 246 ± 20 $km^3$/m.y. in time interval 1 (41.6–39.1 Ma) to 682 ± 61 $km^3$/m.y. (713 $km^3$/m.y. when corrected) in time interval 3 (36.5–33.9 Ma; Figs. 9 and 10). The total volumetric fraction of conglomerate, sand, and fines (finer than sand) released from the Pyrenees can be reconstructed as 8%, 23%, and 69%, respectively, for time interval 1 (Fig. 10A; Table 3). The proportion of fines increased in time interval 2 (5%, 22%, and 73%; Fig. 10B). In time interval 3, considerably more conglomerate and sand were released from the mountain belt, giving a volumetric fraction of conglomerate, sand, and fines of 13%, 27%, and 60% (Fig. 10C). These numbers are significant for two reasons: (1) They give a unique insight into the typical range of time-integrated grain-size distributions of sediment eroded from actively deforming mountain belts, and (2) they show that the variability in total sediment volume released from catchments is not necessarily coupled with the sediment caliber exported from the mountain chain (Whittaker et al., 2011).

Reconstructions of depositional volumes and fluxes suggest that in time interval 1, 116 ± 9 $km^3$/m.y. of sediment supplied to the Escanilla routing system was deposited on the terrestrial wedge top (depositional zones 1–4; Figs. 9A and 10A), whereas 130 ± 11 $km^3$/m.y. bypassed the terrestrial sector and entered the Jaca Basin, representing slightly above 50% of the total initial sediment discharge. Conglomerate was preferentially deposited in the tectonically generated accommodation of the terrestrial sector, leading to a steady decrease in stratigraphic conglomerate fraction, from >50% near the apex of the depositional system to <5% at the terrestrial-marine boundary. Of the 130 ± 11 $km^3$/m.y. of sediment supplied to the terminal phase of the Hecho Group turbidite system in the Jaca Basin, 17% was sand, and 83% was finer than sand. Comparison with the input grain-size distribution therefore shows that preferential extraction of gravel in the terrestrial sector of the routing system left a grain-size distribution that was relatively depleted in gravel and sand, but enriched in fines.

In time interval 2, a flux of 437 ± 34 $km^3$/m.y. of sediment was exported to the Jaca Basin, from a total sediment supply of ~620 ± 48 $km^3$/m.y., a tripling of the starting flux relative to time interval 1. The terrestrial sector of the Escanilla system was strongly oversupplied with sedi-

ment (Fig. 10B). Coarse gravel was extracted from surface fluxes to build stratigraphy with fractions of gravel of >90% in the proximal part of the routing system (Fig. 9B). This is particularly striking because the fraction of gravel in the supply was only 5%, and this underlines the fact that effective prediction of stratigraphy requires coupled constraints on both sediment volume and grain size in the supply, as emphasized by Duller et al. (2010) and Armitage et al. (2011). The fraction of conglomerate preserved as stratigraphy fell to <20% in the Viacamp-Lascuarre area 40 km down-system, but it subsequently increased, along with the sand fraction, downstream of the confluence zone. The percentage of gravel (and sand) in stratigraphy may therefore increase down-system as a result of the resetting effect of a major confluence, and additionally by an increase in bypass in the sector downstream of the confluence. Nevertheless, compared to the input grain-size distribution, preferential extraction of gravel in the terrestrial part of the sediment routing system again left the grain-size distribution supplied to the proximal Jaca Basin relatively depleted in gravel, but with an increase in fines compared to the initial input grain size. Of the 437 ± 34 $km^3$/m.y. of sediment supplied to the Jaca Basin, 20% was sand, and 80% was finer than sand.

In time interval 3, the total sediment supply to the Escanilla system was at least (see * in footnote to Table 3) 682 ± 61 $km^3$/m.y., of which >75% was deposited in the Jaca Basin (Fig. 10C). This total sediment volume is an underestimate due to erosion at the base Oligocene boundary, which would have recycled a volume from time interval 3 into the overlying Antist–Collegats–Upper Campodarbe Group. Sediment supply from Gurb and Sis sources remained almost the same as in time interval 2, but there was a significant supply of sediment from the evolving western Pyrenees via the Santa Orasia tributary. The major increase in the flux of bypassed sediment to this western depocenter is supported by the rapid transition from marine to fluvial environments in the Jaca Basin by time interval 3 (Hogan and Burbank, 1996; Teixell, 1998; Costa et al., 2010). This increase in sediment supply was also accompanied by a significant coarsening in the input grain-size distribution (Fig. 9C), which left stratigraphy enriched in conglomerate and sandstone across the terrestrial sectors of the sediment routing system. Depositional volumes on the wedge top were a factor of >2 larger than during time interval 1, indicating increased accommodation generation but nevertheless continued, strong, sediment overfilling of the terrestrial sector.

The bypass index is calculated as the ratio of the incoming surface sediment flux to the depositional flux in a given basin compartment (Gurb-Pobla and Sis proximal regions, Lascuarre and Viacamp, Ainsa, inner Jaca and outer Jaca). If all of the incoming sediment is deposited in that compartment, the bypass ratio is 1. The ratio varies only slightly between the three time intervals (Fig. 11). In the combined Gurb-Pobla and Sis proximal region, the bypass ratio changes from 9 in time interval 1 to 16 in time interval 2, and 19 in time interval 3, indicating an increasingly strong insufficiency of accommodation space over time. In the fluvial Viacamp-Lascuarre compartment, the bypass index changes from 10 to 24 to 27 from time interval 1 to 2 to 3, showing the same temporal trend, and very strong bypassing of this part of the paleo–sediment routing system. The eastern Ainsa Basin was the location of the coastline during the latest Lutetian and Bartonian. Bypass indices drop to values of 3, 5, and 5 for time intervals 1, 2, and 3, indicating a significant increase in accommodation in this region. The remaining sediment supply was exhausted by deposition in the Jaca Basin. In time intervals 1 and 2, bypass indices fall to ~1 in the inner (eastern) Jaca Basin, rising to 1.2 in time interval 3. In time interval 3, the remaining sediment was deposited in the outer Jaca Basin.

## DISCUSSION

The dynamics of the Escanilla source-to-sink system are illuminated by an evaluation of the long-term volumetric sediment budget and connecting fluxes. Knowledge of this budget allows the evolution of the Pyrenees and its pro-foreland basin systems to be better understood. For example, bedrock thermochronometric data (Fitzgerald et al., 1999; Gibson et al., 2007; Whitchurch et al., 2011; Filleaudeau et al., 2012) suggest an increase in erosion rate in Pyrenean mountain catchments, from ~0.25–0.30 mm/yr in the mid-Eocene to >1 mm/yr in the latest Eocene–Oligocene, leading eventually to the formation of extensive gravel sheets of the Oligocene Collegats-Antist units, which draped and buried the previously active tectonic structures of the wedge-top zone (Coney et al., 1996; Babault et al., 2005; Fillon and van der Beek, 2012). This temporal increase in the sediment released from Pyrenean mountain catchments (Figs. 9 and 10) is recognized in our sediment budget calculations but commences during time interval 2 (36.5–39.1 Ma) in the late Bartonian–early Priabonian. This increase in sediment supply resulted in a chain of events: (1) an increase in conglomerate fraction in the terrestrial segment of the sediment routing system, (2) a westward progradation of the shoreline along the strike of wedge-top structures, (3) much-increased export of sediment to the deep-marine and later fluvial distal depocenters in the west, causing the eventual terrestrialization of the Jaca Basin, and (4) a temporal increase in the bypass index.

A comparison of the sediment budget among three time intervals over the mid- to late Eocene reveals an overall progressive increase in the sediment (including porosity) supplied to the fold-and-thrust belt, from ~250 $km^3$/m.y. to ~620 $km^3$/m.y. to greater than 680 $km^3$/m.y. (713 $km^3$/m.y. corrected for localized erosional truncation). It is speculative whether this resulted from an expansion of catchments toward the main drainage divide of the paleo-Pyrenees or from an increase in erosion rate in the source regions (Allen et al., 2013). Deciphering the relative roles of tectonic shortening and climate change in driving this increasing sediment budget is a goal of future research.

The integrated grain-size fractions, and the downstream partitioning of grain size also vary among the three time intervals. Whereas the sediment supply during time interval 1 consisted of 8% gravel, 23% sand, and 69% fines, time interval 2 saw a reduction of gravel (5%) and increase in fines (74%), and in time interval 3, 13% gravel, 27% sand, and 60% fines were exported from the upland catchments. The grain-size mix supplied from upland catchments is controlled by bedrock lithology, climate, and vegetation, but also by the transient landscape response to tectonic perturbations (Whittaker et al., 2010). It is noteworthy that the changes in the grain-size mix over time are not simply a reflection of the magnitude of the sediment supply, since an increase in supply in time interval 2 is accompanied by a percentage decrease in the release of gravel, whereas a continuing increase in supply in time interval 3 is accompanied by an increase in the proportion of gravel. The variance of grain size in the supply is important in controlling down-system trends in grain-size fining in stratigraphy (Fedele and Paola, 2007; Duller et al., 2010; Michael et al., 2013) and depositional facies and geometries (Strong et al., 2005). The "global" grain-size mix over the 7.7 m.y. duration of the three time intervals in the mid- to late Eocene is 8.8% gravel, 24.5% sand, and 66.7% finer than sand. This "global" figure provides a useful reference that may be applicable to other orogen-foreland basin systems and is a starting point for generic numerical approaches to sediment dispersal.

The generic value of the Escanilla study derives initially from the methodology used to link depositional sinks with erosive source regions in a complex geological context, which requires the use of multiple provenance tools, bedrock and detrital thermochronology, bio-

chronology, and magnetochronology, clast lithology counts, sedimentological logging, and grain-size analysis. These techniques can routinely be applied in other well-preserved fold-and-thrust belt settings, but also in other tectonic contexts such as rifts, passive margins, and cratonic basins. Critically, the sediment routing system fairway must be possible to map, ideally from a combination of surface outcrops and subsurface imagery, and sediment thicknesses must be possible to estimate, so that a volumetric budget can be carried out. Using the exemplar of the source-to-sink approach provided by the Escanilla study, investigations in other tectonic and climatic settings will shed light on challenging generic problems in basin analysis such as the variation of the grain-size mix fluxed out of mountain belts, the nature of downstream fractionation of grain size, the partitioning of sediment volumes in different compartments or segments of the sediment routing system, the downstream variation of the bypass index (ratio of transport flux to depositional flux), and the flux of particulate sediment to the "absorbing states" (Malmon et al., 2003; Allen and Heller, 2012) of the deep sea. All of these problems are key to effective stratigraphic prediction. The sediment budget of a sediment routing system can also be placed in a dimensionless, mass balance framework to enable systems of different scales and fluxes to be compared and contrasted (Paola and Martin, 2012). A mass balance analysis of the Escanilla system is published elsewhere (Michael et al., 2013).

Knowledge of the volumetric budget of geological sediment routing systems and the associated fractionation of grain size is a generic prerequisite for stratigraphic prediction and is the key to understanding the forcing mechanisms for sediment release from upland catchments. We are therefore able to address two important problems: (1) determination of the long-term sediment efflux of upland erosional "engines" that acts as a boundary condition for down-system dispersal (Allen et al., 2013), and (2) the problem highlighted perceptively by Paola (1988, p. 368), that "there is at present no general method for predicting the size distribution of debris supplied to river systems, nor do studies of alluvial basin fill generally provide enough information to reconstruct the supplied distribution." By calculating the sediment budget from source-to-sink and by estimating the grain-size distribution from the entire sediment routing system, we therefore provide quantitative answers to these two problems.

The techniques we outline can be used in the investigation of other geological sediment routing systems where outcrops or subsurface mapping allow the extent of the sediment routing system fairway, from source to sink, to be constrained, and where stratigraphic zonation and correlation are of sufficient resolution for temporal trends in sediment dynamics to be recognized and interpreted. Each stage of the procedure has its own uncertainties, which will vary from case study to case study. Source-to-sink budgets will not be attainable where there is large uncertainty in the teleconnection of distal sinks with proximal feeder systems, and grain-size fractionation trends will not be possible to construct unless there is sufficient outcrop and/or subsurface core coverage to determine bulk grain sizes.

Although the Escanilla is a unique case study, the principles established should be able to be exported to other paleo–sediment routing systems in a range of tectonic and climatic settings, and perhaps to situations of very different bedrock geology and vegetation. The volumetric budget approach might then serve as a powerful tool in forward stratigraphic modeling as well as providing a means of independently assessing the accuracy of catchment erosion rate data derived from thermochronology. Changes in sediment routing system dynamics are likely to have major importance in influencing stratigraphic geometries, facies, and grain-size fractionation at the scale of depositional sequences. Case studies such as the Escanilla therefore are potentially valuable in calibrating sequence stratigraphic studies.

## CONCLUSIONS

A geological (mid- to late Eocene) sediment routing system has been recognized in the prowedge top region of the southern Pyrenees. The Escanilla system connects source regions in the Axial Zone of the south-central Pyrenees with a set of depositional basins accumulating proximal fanglomerates, fluvial, deltaic, and slope sediments, and basin-floor turbidites. These basins were segmented by synsedimentary contractional tectonics, which also shielded the sediment routing system from sediment supplies from the eastern Pyrenees, steered regional sediment dispersal down a regional paleoslope to the west, and deflected sediment transport paths by actively rotating structures associated with lateral-oblique ramps.

The spatial extent of the sediment routing system fairway has been mapped and cross sections constructed at a number of stations in the down-system direction, from which the total volume of deposited sediment from source to sink has been estimated. The cumulative depositional volume in the down-system direction allows the surface flux and the depositional flux to be estimated, together with their ratio the bypass index. Sedimentological logs were used to calculate the abundance of three grain-size fractions at each station, from which the "global" grain-size mix of the supply could be obtained.

Comparison of the sediment budget among three time intervals over the mid- to late Eocene reveals an overall progressive increase in the sediment (including porosity) supplied by the source regions in the high Pyrenees, from ~250 $km^3$/m.y. to ~620 $km^3$/m.y. to greater than 680 $km^3$/m.y. (713 $km^3$/m.y. corrected for localized erosional truncation). The increasing supply over time drove strong westward progradation and the eventual terrestrialization of the down-system Jaca Basin.

The sediment supply during time interval 1 consisted of 8% gravel, 23% sand, and 69% fines, whereas time interval 2 saw a reduction of gravel (5%) and increase in fines (74%), and in time interval 3, 13% gravel, 27% sand, and 60% fines were exported from the upland catchments. The "global" grain-size mix over the 7.7 m.y. duration of the three time intervals in the mid- to late Eocene is 8.8% gravel, 24.5% sand, and 66.7% finer than sand. The secular increase in the sediment supply therefore did not have a simple linear relationship with its grain-size mix.

The downstream partitioning of grain-size fractions shows a sensitive response to patterns of accommodation generation and the grain-size mix of the supply. The downstream variation of the bypass index for time intervals 1 and 2 shows a decrease in bypass in the coastal and marine environments of the western Ainsa and Jaca Basins, which pinned the gravel front. During time interval 3, the same down-system pattern of bypass occurred, but gravel extended into the fluvial environments of the inner Jaca Basin.

Case studies such as this illustrate the functioning of sediment routing systems at geological time scales (~2 m.y.). The Escanilla study provides an example for other case studies involving different tectonic and climatic settings and basin dynamics, gives valuable input data for forward stratigraphic models, and serves as a calibration tool for sequence stratigraphic studies.

### ACKNOWLEDGMENTS

We gratefully acknowledge Statoil for funding to Allen and ARAMCO for a scholarship to Michael. Our work benefited from the input of Cai Puigdefàbregas (CSIC [Consejo Superior de Investigaciones Científicas] Barcelona), Jaume Vergés (CSIC Barcelona), Bet Beamud (University of Barcelona), Stephen Vincent (CASP [Cambridge Arctic Shelf Programme]), Hugh Sinclair (Edinburgh), and Robert Duller (Liverpool University). We also thank Andrew Parsons, who collaborated in field work in the Sis area. We also gratefully acknowledge the detailed comments of two anonymous journal reviewers and editor Rebecca Dorsey.

**REFERENCES CITED**


Allen, P.A., 2008a, From landscapes into geological history: Nature, v. 451, p. 274–276, doi:10.1038/nature06586.

Allen, P.A., 2008b, Time scales of tectonic landscapes and their sediment routing systems, *in* Gallagher, K., Jones, S.J., and Wainwright, J., eds., Landscape Evolution: Denudation, Climate and Tectonics over Different Time and Space Scales: Geological Society of London Special Publication 296, p. 2–28.

Allen, P.A., and Allen, J.R., 2013, Basin Analysis: Principles and Application to Petroleum Play Assessment: Oxford, UK, Wiley-Blackwell, 624 p.

Allen, P.A., and Heller, P.L., 2012, The timing, distribution and significance of tectonically generated gravels in terrestrial sediment routing systems, *in* Busby, C., and Azor Pérez, A., eds., Tectonics of Sedimentary Basins, Recent Advances: Oxford, UK, Wiley-Blackwell, p. 111–130.

Allen, P.A., Cabrera, L., Colombo, F., and Matter, A., 1983, Variations in fluvial style on the Eocene–Oligocene alluvial fan of the Scala Dei Group, SE Ebro Basin, Spain: Journal of the Geological Society of London, v. 140, p. 133–146, doi:10.1144/gsjgs.140.1.0133.

Allen, P.A., Armitage, J.J., Carter, A., Duller, R.A., Michael, N.A., Sinclair, H.D., Whitchurch, A.L., and Whittaker, A.C., 2013, The Qs problem: Sediment volumetric balance of proximal foreland basin systems, *in* Föllmi, K.B., Schlunegger, F., and Weissert, H., Alpine Sedimentology: Special Issue in Honour of Albert Matter and Daniel Bernoulli: Sedimentology, v. 60, p. 102–130, doi:10.1111/sed.12015.

Armitage, J.J., Duller, R.A., Whittaker, A.C., and Allen, P.A., 2011, Transformation of tectonic and climatic signals from source to sedimentary archive: Nature Geoscience, v. 4, p. 231–235, doi:10.1038/ngeo1087.

Babault, J., Van den Driessche, J., and Bonnet, S., 2005, Origin of the highly elevated Pyrenean peneplain: Tectonics, v. 24, TC2010, doi:10.1029/2004TC001697.

Beamud, E., 2013, Paleomagnetism and Thermochronology in Tertiary Syntectonic Sediments of the South-Central Pyrenees: Chronostratigraphy, Kinematics and Exhumation Constraints [Ph.D. thesis]: Barcelona, Spain, University of Barcelona, 250 p.

Beamud, E., Garcés, M., Cabrera, L., Muñoz, J.A., and Almar, Y., 2003, A new middle to late Eocene continental chronostratigraphy from NE Spain: Earth and Planetary Science Letters, v. 216, p. 501–514, doi:10.1016/S0012-821X(03)00539-9.

Beamud, E., Muñoz, J.A., Fitzgerald, P.G., Baldwin, S.L., Garcés, M., Cabrera, L., and Metcalf, J.R., 2010, Magnetostratigraphy and detrital apatite fission track thermochronology in syntectonic conglomerates: Constraints on the exhumation of the south-central Pyrenees: Basin Research, v. 13, no. 3, p. 309–331, doi:10.1111/j.1365-2117.2010.00492.x.

Beaumont, C., Muñoz, J.A., Hamilton, J., and Fullsack, P., 2000, Factors controlling the Alpine evolution of the central Pyrenees inferred from a comparison of observations and geodynamical models: Journal of Geophysical Research, v. 105, p. 8121–8145, doi:10.1029/1999JB900390.

Bentham, P., 1992, The Tectonic Stratigraphic Development of the Western Oblique Ramp of the South-Central Pyrenean Thrust System, North Spain [Ph.D. thesis]: Los Angeles, California, University of Southern California, 253 p.

Bentham, P., and Burbank, D.W., 1996, E13 chronology of Eocene foreland basin evolution along the western margin of the south-central Pyrenees, *in* Friend, P.F., and Dabrio, C.J., eds., Tertiary Basins of Spain: The Stratigraphic Record of Crustal Kinematics: Cambridge, UK, Cambridge University Press, p. 144–152.

Bentham, P.A., Burbank, D.W., and Puigdefabregas, C., 1992, Temporal and spatial controls on alluvial architecture in an axial drainage system, Upper Eocene Campodarbe Group, southern Pyrenean foreland basin, Spain: Basin Research, v. 4, p. 335–352, doi:10.1111/j.1365-2117.1992.tb00052.x.

Bentham, P.A., Talling, P.J., and Burbank, D.W., 1993, Braided stream and flood-plain deposition in a rapidly aggrading basin: The Escanilla formation, Spanish Pyrenees, *in* Best, J.L., and Bristow, C.S., eds., Braided Rivers: Geological Society London Special Publication 75, p. 177–194, doi:10.1144/GSL.SP.1993.075.01.11.

Burbank, D.W., and Vergés, J., 1994, Reconstruction of topography and related depositional systems during active thrusting: Journal of Geophysical Research, v. 99, p. 20,281–20,297, doi:10.1029/94JB00463.

Burbank, D.W., Meigs, A., and Brozovic, N., 1996, Interactions of growing folds and coeval depositional systems: Basin Research, v. 8, p. 199–223, doi:10.1046/j.1365-2117.1996.00181.x.

Carvajal, C., and Steel, R., 2012, Source-to-sink sediment volumes within a tectono-stratigraphic model for a Laramide shelf-to-deep-water basin: Methods and results, *in* Busby, C., and Azor Pérez, A., eds., Tectonics of Sedimentary Basins: Recent Advances: Oxford, UK, Blackwell Publishing, p. 131–151.

Castelltort, S., and Van Den Driessche, J., 2003, How plausible are high frequency sediment supply–driven cycles in the stratigraphic record?: Sedimentary Geology, v. 157, p. 3–13, doi:10.1016/S0037-0738(03)00066-6.

Colombo, F., 1980, Estratigrafia y Sedimentologia del Terciario Interior Continental de los Catalanides [Ph.D. thesis]: Barcelona, Spain, University of Barcelona, 291 p.

Coney, P.J., Muñoz, J.A., McClay, K.R., and Evenchick, C.A., 1996, Syntectonic burial and post-tectonic exhumation of the southern Pyrenees foreland fold-thrust belt: Journal of the Geological Society of London, v. 153, p. 9–16, doi:10.1144/gsjgs.153.1.0009.

Costa, E., Garcés, M., López-Blanco, M., Beamud, E., Gómez-Paccard, M., and Larrasoaña, J.C., 2010, Closing and continentalization of the South Pyrenean foreland basin (NE Spain): Magnetochronological constraints: Basin Research, v. 22, p. 904–917, doi:10.1111/j.13652117.2009.00452.x.

Costa, E., Garcés, M., López-Blanco, M., Serra-Kiel, J., Bernaola, G., Cabrera, L., and Beamud, E., 2013, The Bartonian-Priabonian marine record of the eastern South Pyrenean Foreland Basin (NE Spain): A new calibration of the larger foraminifers and calcareous nannofossil zonation: Geologica Acta, v. 11, p. 177–193.

Covault, J.A., Romans, B.W., Fildani, A., McGann, M., and Graham, S.A., 2010, Rapid climate signal propagation from source to sink in a southern California sediment-routing system: The Journal of Geology, v. 118, p. 247–259, doi:10.1086/651539.

Cross, T.A., and Lessinger, M.A., 1988, Sediment volume partitioning: Rationale for stratigraphic model evaluation and high-resolution stratigraphic correlation, *in* Gradstein, F., Sandvik, K., and Milton, N., eds., Sequence Stratigraphy: Concepts and Applications: Norwegian Petroleum Society Special Publication 8, p. 171–195.

Cuevas-Gonzalo, M.C., 1989, Sedimentary Facies and Sequential Architecture of Tide-Influenced Alluvial Deposits, an Example from the Middle Eocene Capella Formation, South-Central Pyrenees, Spain [Ph.D. thesis]: Instituut voor Aardwetenschappen der Rijksuniversiteit Utrecht, Geologica Ultraiectina, v. 61, p. 1–152.

Densmore, A.L., Allen, P.A. and Simpson, G., 2007, Development and response of a coupled catchment-fan system under changing tectonic and climatic forcing: Journal of Geophysical Research–Earth Surface, v. 112, F01002, doi:10.1029/2006JF000474.

Dreyer, T., Corregidor, J., Arbues, P., and Puigdefabregas, C., 1999, Architecture of the tectonically influenced Sobrarbe deltaic complex in the Ainsa Basin, northern Spain: Sedimentary Geology, v. 127, no. 3–4, p. 127–169, doi:10.1016/S0037-0738(99)00056-1.

Duller, R.A, Whittaker, A.C., Fedele, J.J., Springett, J., Smithells, R., and Allen, P.A., 2010, From grain size to tectonics: Journal of Geophysical Research–Earth Surface, v. 115, F03022, doi:10.1029/2009JF001495.

Fedele, J.J., and Paola, C., 2007, Similarity solutions for fluvial sediment fining by selective deposition: Journal of Geophysical Research, v. 112, F02038, doi:10.1029/2005JF000409.

Filleaudeau, P.Y., Mouthereau, F., and Pik, R., 2012, Thermotectonic evolution of the south-central Pyrenees from rifting to orogeny: Insights from detrital zircon U/Pb and (U-Th)/He thermochronometry: Basin Research, v. 24, p. 401–417, doi:10.1111/j.1365-2117.2011.00535.x.

Fillon, C., and van der Beek, P., 2012, Post-orogenic evolution of the southern Pyrenees: constraints from inverse thermo-kinematic modelling of low-temperature thermochronology data: Basin Research, v. 24, no. 4, p. 418–436, doi:10.1111/j.1365-2117.2011.00533.x.

Fitzgerald, P., Munoz, J.A., Coney, P., and Baldwin, S.L., 1999, Asymmetric exhumation across the central Pyrenees: Implications for the tectonic evolution of a collisional orogen: Earth and Planetary Science Letters, v. 173, p. 157–170, doi:10.1016/S0012-821X(99)00225-3.

Garcia-Castellanos, D., Vergés, J., and Cloetingh, S., 2003, Interplay between tectonics, climate and fluvial transport during the Cenozoic evolution of the Ebro Basin (NE Iberia): Journal of Geophysical Research, v. 108, no. B7, 2347, doi:10.1029/2002JB002073.

Gibson, M., Sinclair, H.D., Lynn, G.J., and Stuart, F.M., 2007, Late- to post-orogenic exhumation of the central Pyrenees revealed through combined thermochronological data and modelling: Basin Research, v. 19, p. 323–334, doi:10.1111/j.1365-2117.2007.00333.x.

González-Bonorino, G., Colombo, F., and Abascal, L., 2010, Architecture of an Oligocene fluvial ribbon sandstone in the Ebro Basin, north-eastern Spain: Sedimentology, v. 57, p. 845–856, doi:10.1111/j.1365-3091.2009.01122.x.

Gradstein, F.M., and Ogg, J.G., 2004, Geological timescale 2004, Why, how and where next!: Lethaia, v. 37, p. 175–181.

Gradstein, F.M., Ogg, J.G., and Smith, A., 2004, A Geologic Time Scale 2004: Cambridge, UK, Cambridge University Press, 589 p.

Hogan, P., and Burbank, D., 1996, Evolution of the Jaca piggyback basin and emergence of the External Sierra, southern Pyrenees, *in* Friend, P.F., and Dabrio, C.J., eds., Tertiary Basins of Spain: The Stratigraphic Record of Crustal Kinematics: Cambridge, UK, Cambridge University Press, p. 144–152.

Holl, J.E., and Anastasio, D.J., 1993, Paleomagnetically derived folding rates, southern Pyrenees, Spain: Geology, v. 21, p. 271, doi:10.1130/0091-7613(1993)021<0271:PDFRSP>2.3.CO;2.

Jolley, E.J., 1987, Thrust Tectonics and Alluvial Architecture of the Jaca Basin, Southern Pyrenees [Ph.D. thesis]: Cardiff, University of Wales.

Kim, W., Connell, S.D., Steel, E., Smith, G.A., and Paola, C., 2011, Mass-balance control on the interaction of axial and transverse channel systems: Geology, v. 39, p. 611–614, doi:10.1130/G31896.1.

Labourdette, R., and Jones, R.R., 2007, Characterization of fluvial architectural elements using a three-dimensional outcrop data set: Escanilla braided system, south-central Pyrenees, Spain: Geosphere, v. 3, p. 422, doi:10.1130/GES00087.1.

López-Blanco, M., Marzo, M., Burbank, D.W., Vergés, J., Roca, E., Anadón, P., and Piña, J., 2000, Tectonic and climatic controls on the development of foreland fan deltas: Montserrat and Sant Llorenç del Munt systems (Middle Eocene, Ebro Basin, NE Spain): Sedimentary Geology, v. 138, p. 17–39, doi:10.1016/S0037-0738(00)00142-1.

López-Blanco, M., Marzo, M., and Muñoz, J.-A., 2003, Low-amplitude, syn-sedimentary folding of a deltaic complex: Roda Sandstone (lower Eocene), South Pyrenean Foreland Basin: Basin Research, v. 15, p. 73–95.

Malmon, D.V., Dunne, T., and Reneau, S.L., 2003, Stochastic theory of particle trajectories through alluvial valley floors: The Journal of Geology, v. 111, p. 525–542, doi:10.1086/376764.

Marr, J.G., Swenson, J.B., Paola, C., and Voller, V.R., 2000, A two-diffusion model of fluvial stratigraphy in closed depositional basins: Basin Research, v. 12, p. 381–398, doi:10.1046/j.1365-2117.2000.00134.x.

Mellere, D., 1993, Thrust-generated, back-fill stacking of alluvial fan sequences, south-central Pyrenees, Spain (La Pobla de Segur Conglomerates), *in* Frostick, L.E., and Steel, R.J., eds., Tectonic Controls and Signatures in Sedimentary Successions: International Association Sedimentologists Special Publication 20, p. 259–276.

Mellere, D., and Marzo, M., 1992, Los depósitos aluviales sintectónicos de la Pobla de Segur: Alogrupos y su significado tectonoestratigráfico: Acta Geologica Hispanica, v. 27, p. 145–159.

Michael, N.M., 2013, Functioning of an Ancient Sediment Routing System, the Escanilla Formation, South-Central Pyrenees [Ph.D. thesis]; London, UK, Imperial College London 286 p.

Michael, N.M., Whittaker, A.C., and Allen, P.A., 2013, The functioning of sediment routing systems using a mass balance approach: Example from the Eocene of the southern Pyrenees: The Journal of Geology, v. 121, p. 581–606, doi:10.1086/673176.

Mochales, T., Casas, A.M., Pueyo, E.L., and Barnolas, A., 2012, Rotational velocity for oblique structures (Boltaña anticline, southern Pyrenees): Journal of Structural Geology, v. 35, p. 2–16, doi:10.1016/j.jsg.2011.11.009.

Muñoz, J.A., 1992, Evolution of a continental collision belt: ECORS-Pyrenees crustal balanced cross-section, *in* McClay, K., ed., Thrust Tectonics: London, Chapman and Hall, p. 235–246.

Muñoz, J.A., Beamud, E., Fernández, O., Arbués, P., Dinarès-Turell, J., and Poblet, J., 2013, The Ainsa Fold and Thrust Oblique Zone: Kinematics of a curved contractional system from paleomagnetic and structural data: Tectonics, v. 32, p. 1142–1175, doi:10.1002/tect.20070.

National Aeronautics and Space Administration (NASA) and Japan ASTER Program, 2011, ASTER scenes, ASTGDEMV2_0N 41E001, N41E000, N41 W001, N 42E001, N42E000, N42 W001, N42 W002, N 43E001, N43E000, N43 W001, N43 W002: http://earthexplorer.usgs.gov (accessed 5 January 2011).

Nijman, W., 1998, Cyclicity and basin axis shift in a piggyback basin: Towards modelling of the Eocene Tremp-Ager Basin, South Pyrenees, Spain, *in* Mascle, A., Puigdefàbregas, C., Luterbacher, H.P., and Fernández, M., eds., Cenozoic Foreland Basins of Western Europe: Geological Society of London Special Publication 134, p. 135–162, doi:10.1144/GSL.SP.1998.134.01.07.

Paola, C., 1988, A simple basin-filling model for coarse-grained alluvial systems, *in* Cross, T.A., ed., Quantitative Dynamic Stratigraphy: Englewood Cliffs, New Jersey, Prentice-Hall, p. 363–374.

Paola, C., and Martin, J., 2012, Mass balance effects in depositional systems: Journal of Sedimentary Research, v. 82, p. 435–450, doi:10.2110/jsr.2012.38.

Paola, C., Heller, P.L., and Angevine, C.L., 1992, The large-scale dynamics of grain size variation in alluvial basins. 1. Theory: Basin Research, v. 4, p. 73–90, doi:10.1111/j.1365-2117.1992.tb00145.x.

Parsons, A.J., Michael, N.A., Whittaker, A.C., Duller, R.A., and Allen, P.A., 2012, Grain size trends reveal the late orogenic tectonic and erosional history of the south-central Pyrenees, Spain: Journal of the Geological Society of London, v. 169, p. 111–114, doi:10.1144/0016-76492011-087.

Puigdefàbregas, C., 1975, La sedimentacion molásica en la cuenca de Jaca: Pirineos, v. 104, p. 188.

Puigdefàbregas, C., and Souquet, P., 1986, Tecto-sedimentary cycles and depositional sequences of the Mesozoic and Tertiary from the Pyrenees, *in* Banda, E., and Wickhan, S.W., eds., The Geological Evolution of the Pyrenees: Tectonophysics, v. 129, p. 173–203.

Puigdefàbregas, C., Muñoz, J.A., and Vergés, J., 1992, Thrusting and foreland basin evolution in the southern Pyrenees, *in* McClay, K.R., ed., Thrust Tectonics: London, Chapman & Hall, p. 247–254.

Ramos, E., Busquets, P., and Vergés, J., 2002, Interplay between longitudinal fluvial and transverse alluvial fan systems and growing thrusts in a piggyback basin (SE Pyrenees): Sedimentary Geology, v. 146, p. 105–131, doi:10.1016/S0037-0738(01)00169-5.

Rodríguez-Pintó, A., Pueyo, E.L., Serra-Kiel, J., Samsó, J.M., Barnolas, A., and Pocoví, A., 2012, Lutetian magnetostratigraphic calibration of larger foraminifera zonation (SBZ) in the southern Pyrenees: Palaeogeography, Palaeoclimatology, Palaeoecology, v. 333–334, p. 107–120, doi:10.1016/j.palaeo.2012.03.012.

Sáez, A., Anadón, P., Herrero, M.J., and Moscariello, A., 2007, Variable style of transition between Paleogene fluvial fan and lacustrine systems, southern Pyrenean foreland, NE Spain: Sedimentology, v. 54, p. 367–390, doi:10.1111/j.1365-3091.2006.00840.x.

Séguret, M., 1969, Tectonics of southern Pyrenees style and role of displacement towards south of Secondary and Tertiary series of central part of southern slope of Pyrenees: Comptes Rendus Hebdomadaires des Séances de l'Académie des Sciences, ser. D, Sciences Naturelles, v. 268, no. 6, p. 907.

Sinclair, H.D., Gibson, M., Naylor, M., and Morris, R.G., 2005, Asymmetric growth of the Pyrenees revealed through measurement and modeling of orogenic fluxes: American Journal of Science, v. 305, p. 369–406, doi:10.2475/ajs.305.5.369.

Somme, T.O., Piper, D.J.W., Deptuck, M.E., and Helland-Hansen, W., 2011, Linking onshore-offshore sediment dispersal in the Golo source-to-sink system (Corsica, France) during the late Quaternary: Journal of Sedimentary Research, v. 81, p. 118–137, doi:10.2110/jsr.2011.11.

Strong, N., Sheets, B., Hickson, T., and Paola, C., 2005, Mass balance framework for quantifying downstream changes in fluvial architecture, *in* Blum, M.D., Marriott, S.B., and Leclair, S.F., eds., Fluvial Sedimentology VII: International Association of Sedimentologists Special Publication 35, p. 243–253, doi:10.1002/9781444304350.ch14.

Teixell, A., 1998, Crustal structure and orogenic material budget in the west central Pyrenees: Tectonics, v. 17, p. 395–406, doi:10.1029/98TC00561.

Turner, J.P., 1992, Evolving alluvial stratigraphy and thrust front development in the west Jaca piggyback basin, Spanish Pyrenees: Journal of the Geological Society of London, v. 149, p. 51–63, doi:10.1144/gsjgs.149.1.0051.

Vergés, J., 2007, Drainage responses to oblique and lateral thrust ramps: A review, *in* Nichols, G., Williams, E., and Paola, C., eds., Sedimentary Processes, Environments and Basins: A Tribute to Peter Friend: International Association Sedimentologists Special Publication 38, p. 29–47, doi:10.1002/9781444304411.ch3.

Vergés, J., and Burbank, D.W., 1996, Eocene-Oligocene thrusting and basin configuration in the eastern and central Pyrenees (Spain), *in* Friend, P.F., and Dabrio, C.J., eds., Tertiary Basins of Spain: Cambridge, UK, Cambridge University Press, p. 120–133.

Vergés, J., Millán, H., Roca, E., Muñoz, J.A., Marzo, M., Cirés, J., Den Bezemer, T., Zoetemeijer, R., and Cloetingh, S., 1995, Eastern Pyrenees and related foreland basins: Pre-, syn- and post-collisional crustal-scale cross-sections: Marine and Petroleum Geology, v. 12, no. 8, p. 903–915, doi:10.1016/0264-8172(95)98854-X.

Vincent, S.J., 1993, Fluvial Palaeovalleys in Mountain Belts: An Example from South-Central Pyrenees [Ph.D. thesis]: Liverpool, UK, University of Liverpool, 407 p.

Vincent, S.J., 2001, The Sis palaeovalley: A record of proximal fluvial sedimentation and drainage basin development in response to Pyrenean mountain building: Sedimentology, v. 48, p. 1235–1276, doi:10.1046/j.1365-3091.2001.00421.x.

Whitchurch, A., Carter, A., Sinclair, H.D., Duller, R., Whittaker, A.C., and Allen, P.A., 2011, Sediment routing systems and the lag-time concept: A case study from the southern Pyrenees: American Journal of Science, v. 311, p. 442–482, doi:10.2475/04.2011.00.

Whittaker, A.C., Attal, M., and Allen, P.A., 2010, Characterising the origin, nature and fate of sediment exported from catchments perturbed by active tectonics: Basin Research, v. 22, p. 809–828, doi:10.1111/j.1365-2117.2009.00447.x.

Whittaker, A.C., Duller, R.A., Springett, J., Smithells, R., Whitchurch, A.L., and Allen, P.A., 2011, Decoding downstream trends in stratigraphic grain-size as a function of tectonic subsidence and sediment supply: Geological Society America Bulletin, v. 123, p. 1363–1382, doi:10.1130/B30351.1.

Science Editor: Christian Koeberl
Associate Editor: Rebecca Dorsey

Manuscript Received 28 June 2013
Revised Manuscript Received 23 October 2013
Manuscript Accepted 6 December 2013

Printed in the USA